Influence of combined impact and cyclic loading on the overall fatigue life of forged steel, EA4T

Malekzadeh, A, Hadidimoud, S & Farhangdoost, K

Original citation & hyperlink:
Malekzadeh, A, Hadidimoud, S & Farhangdoost, K 2017, 'Influence of combined impact and cyclic loading on the overall fatigue life of forged steel, EA4T' *Journal of Mechanical Science and Technology*, vol 31, no. 3, pp. 1097-1103
https://dx.doi.org/10.1007/s12206-016-0923-x

DOI 10.1007/s12206-016-0923-x
ISSN 1738-494X
ESSN 1976-3824

Publisher: Springer

The final publication is available at Springer via http://dx.doi.org/10.1007/s12206-016-0923-x

Influence of combined impact and cyclic loading on the overall fatigue life of forged steel, EA4T

A. Malekzadeh[1], S. Hadidi-Moud[1], Kh. Farhangdoost[1]

[1] *Department of Mechanical Engineering, Ferdowsi University of Mashhad, Mashhad, Iran*

Abstract

The performance of forged steel, *EA4T*, used in rail industry, under simulated in service conditions, i.e. combined impact - cyclic loading, was investigated through a comprehensive experimental programme. The standard Paris-Erdogan fatigue design curve parameters, *m* and *C*, were calibrated to account for the effect of the impact component of loading. A minimum threshold for impact load component, identified in the experiments, was also incorporated in the proposed empirical model. Comparison with experimental findings indicated that this "modified" Fatigue design curve could predict the fatigue life of pre-impact loaded specimens with sufficient accuracy. It was therefore, suggested that the modified model may be used as a novel design tool for predicting the overall fatigue life of components made of this material under the specified combined impact and fatigue loading conditions.

Keywords: Combined impact-fatigue; Impact threshold; Modified Paris-Erdogan; Forged steel *EA4T*

1. Introduction

Fatigue fracture is the most common cause of failure of components and structures, specifically those made of various grades of steel. Investigating the performance and their response to cyclic loading has been the focus of an enormous portion of research in this field during the last few decades. Extensive data has been acquired, mostly in the form applicable to the validation and calibration of the parameters of the Paris law for safe life prediction of the cases of interest. Moreover, considerable attention has been paid to investigate the effects associated with the variation of loading conditions such as frequency, amplitude, and the rate of loading. Experimental findings also demonstrated that under normal working conditions frequencies up to around 400 Hz did not affect the endurance limit of steel specimens. However, the endurance limit at higher frequencies, where the time for a load cycle was reduced to a few micro seconds (this is the case under impact loading) was much higher than that at frequencies up to 400 Hz. This observation have been linked to the simultaneous contribution of the increasing strain rate, and increasing temperature due to deformation mechanisms at the micro-scale [1]. Also, results corresponding to the conventional fatigue loading regimes, indicated that increasing the load amplitude (i.e. the stress ratio effect) at room temperature introduced a shift onto the standard Paris–Erdogan fatigue curve [2, 3] (on the *da/dN* versus *ΔK* diagram).

The spectrum of impact load is composed of a high amplitude peak followed by lower level tension and compression [4]. It means that in the impact loading stress ratio (*R*) value is lower than it is in the non-impact loading condition. The fatigue life is seen to be highly dependent on the *R* value [5].

Additionally, numerous investigations have been carried out with the objective of estimating the material behavior under "impact-fatigue" loading condition. In "impact-fatigue", because of the strain-rate, steel specimens exhibit an unusually high yield stress, ultimate tensile strength, and ductile to brittle transition temperature. In general, it is believed that the "impact-fatigue" strength is higher than the conventional fatigue strength [6].

Stanton and Bairstow [7] and McAdam [8] plotted the energy absorbed per impact, E_i, against the number of impacts to failure, N_f. The resulting $(E_i - E_f)$ curves were found to be similar in shape to the conventional S-N curves obtained in fatigue experiments. Johnson *et al* [9, 10] showed that high cycle impact fatigue was governed by the following equation:

$$E_i = E_0 + mN_f^{-q}$$

where E_i is the energy absorbed per impact, E_0 is the impact fatigue limit, N is the number of impacts to failure, and m and q are known as the impact fatigue parameter and impact fatigue exponent, respectively.

Particularly, impact loads cannot, a priori, be represented, with validity, by a simple constant amplitude sinusoid. The real loading condition is significantly more complicated than the simple loading of laboratory test conditions.

In general, depending on the loading rate and the imposed energy, both microscopic and macroscopic properties of metallic materials may be affected by the impact loading. Standard impact tests such as Charpy use strain rate in the range of $10^1 \sim 10^3 s^{-1}$ [6], substantially higher than the rates applied in conventional fatigue tests. Experimental investigation of the effects of impact loading is therefore limited to the test machine facilities [11, 12].

The influence of impact loading on estimating the fatigue characteristics in components subjected to combined impact and fatigue loading is unclear. Variation of stress intensity

factor, ΔK, as the main characteristic parameter of fatigue fracture [13], was correlated to the crack growth under cyclic loading by Paris–Erdogan law [14]. Due to the importance of the combined loading conditions (i.e. impact loading followed by fatigue load) considerable attention has been paid to explore the behavior of the forged steel of interest subjected to the combination of these loading mechanisms by maintaining the use of Paris–Erdogan equation. This is especially linked to the use of forged steels in the civil sector including the railway and mining industries as well as in many military applications. The response of forged steel components to such combination of loading conditions plays an increasingly important role in their suitability for intended industrial applications.

In this paper the contribution of impact loading to subsequent fatigue fracture is modeled by use of modified Paris–Erdogan constants *C* and *m*. The findings of an extensive experimental program were used to achieve this purpose. Paris–Erdogan constants, *m* and *C*, were modified by calibrating the Paris–Erdogan equation based on validated test data.

2. Experimental program

In rail industry, the rail, the wheels and the axels are subjected to regular cyclic loading as well as occasional impact loads of various sources. One area of practical application of the model proposed in present study is to obtain more reliable estimation of the service life for these components. Therefore, a suitable material with wide application in the rail industry was procured for the testing program.

2.1 *material and specimens*

The material selected for the study was forged steel EA4T used in railway industry mostly for fabrication of axles. The Mechanical properties and composition of the steel were measured according to ASTM standards E0008M-08 [16] and E2248-09 [16] as summarized in tables 1 and 2 respectively.

The fabrication and preparation of bend specimens SE (B), followed the procedures of *ASTM E399* standard [17]. Details and geometry of standard tests specimens are shown in Fig. 1.

Table1
Mechanical properties of the specimens

Yield Strength(N/mm^2)	Tensile Strength(N/mm^2)	Elongation (%)	Impact Energy U(J)
480	620 - 630	25	16

Table2
Chemical properties of the specimens (% W)

Fe	Ni	Mo	Cu	Cr	Mn	Si	C
97.7	0.125	0.035	00.159	0.14	0.92	0.4	0.38

Table3
Specimen groups

Groups	1	2	3	4	5	6	7	8	9
Input energy(J	0.5	0.8	1.0	1.3	1.6	2.0	2.3	2.6	3

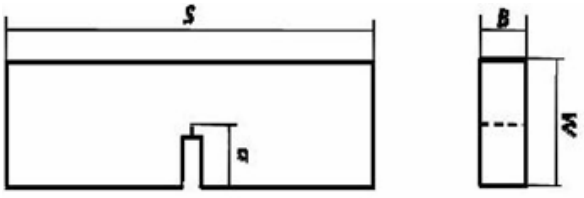

Fig. 1. Geometry and dimensions of the test specimens, (B, W, S, a) = 0.005, 0.01, 0.04, 0.005 (m).

2.2 *Experimental procedures*

A test plan for combined loading was designed based on trial tests to identify the range of prior loads of each type that would affect the subsequent response of the specimen to the latter. Trial tests were also performed to identify the threshold levels (i.e. the maximum load levels that had no effect on the test piece performance) for each type of loading. Tests of "fatigue only" as well as "impact only", were also carried out to identify the extreme situations within the practical load range. To cover the whole range of impact load component for combined loading experiments, nine series of the specimens, five test pieces each, were fabricated according to the *ASTM* standards. These are summarized in Table 3.

The impact energy applied to the specimens range from 0.5 to 3 Jules.

A drop weight type impact test rig was designed and fabricated for this purpose. This small-scale apparatus, shown in Fig. 2 enabled the application of predefined energy levels. The impact loads were applied according to ASTM *E0008M-08* standard [18].

The strain rate was in the range of 10^1-10^3 s^{-1}. For all impact loads, Fatigue loading followed the procedures out lend in *ASTM E399* standard. All tests were carried out in room temperature conditions, i.e. typically 20°C.

For all specimens, the crack tip opening displacement, *CTOD*, was measured after the application of predefined impact energy. These measurements followed the *ASTM E1290-93* standard [19]. The same fatigue loads were then applied to all groups of pre-impact loaded specimens. These loads were also identified from the trial tests that were specifically conducted for this purpose, to ensure all specimens including those subjected to the minimum impact as well as those absorbed the maximum impact energy would withstand a considerable number of fatigue load cycles before final fracture occurred. The characteristics of fatigue loads, maximum and minimum amplitude as well as frequency of loading are presented in table 4.

Table4
Fatigue loading characteristic for pre-impact loaded specimens

P_{mean}(N)	P_{amp}(N)	F (Hz)
500	450	20

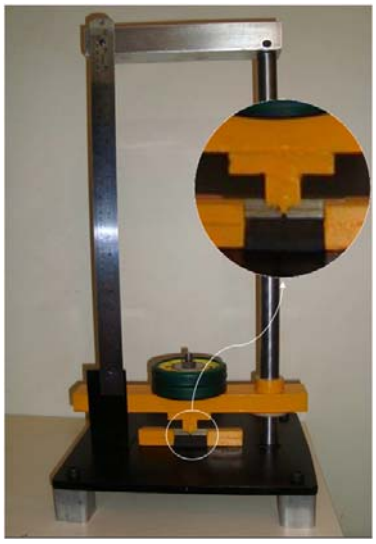

Fig. 2. Test rig machine for applying definite impact energy to SE (B) specimen

Using the procedures of *ASTM E399*, equations (1) to (4) were used to calculate the corresponding stress intensity factors after the application of fatigue loads. The non-dimensional geometry factor a/w represents the geometry of the specific *SE (B)* specimens used in this experimental study.

$$u = \frac{1}{1+\sqrt{\frac{E.B_e.V_m}{P}\left(\frac{4W}{S}\right)}} \quad (1)$$

$$B_e = B - (B - B_N)^2/B \quad (2)$$

$$\frac{a}{w} = 1 - 3.95u + 2.982u^2 - 3.214u^3 + 51.516u^4 - 113.031u^5 \quad (3)$$

$$f\left(\frac{a}{W}\right) = 3\sqrt{\frac{a}{W}} \cdot \frac{1.99 - \left(\frac{a}{W}\right)\left(1-\frac{a}{W}\right)\left[2.15 - 3.93\left(\frac{a}{W}\right) + 2.7\left(\frac{a}{W}\right)^2\right]}{4\left(0.8 + \frac{a}{W}\right)\left(1-\frac{a}{W}\right)^{(3/2)}} \quad (4)$$

$$K = \frac{P_Q \cdot S}{\sqrt{B B_N} W^{\frac{3}{2}}} \cdot f\left(\frac{a}{W}\right) \quad (5)$$

Where P_Q and P are forces (N), B is the specimen thickness (m), B_N refers to the specimen thickness between the roots of the side grooves (m), S is the span (m), W is specimen width (depth) (m), a is crack size (m), and V_m represents the crack mouth opening displacement, *CTOD* (m).

Results obtained from the experiments are shown in Fig 3 from which it is evident that, as expected, the variation of impact loads has resulted in significant change in the corresponding stress intensity factors.

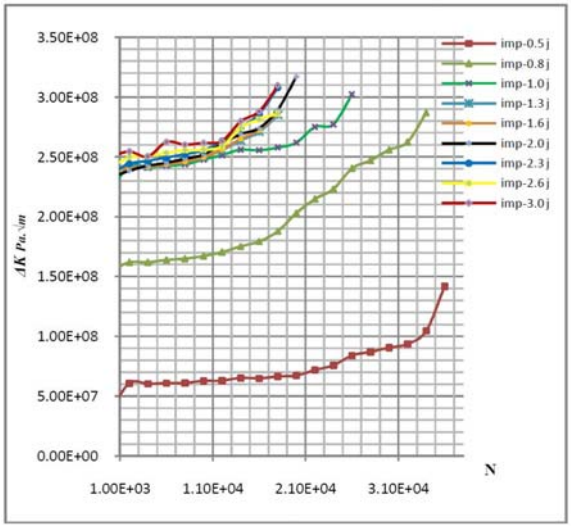

Fig 3. Stress intensity factor on fatigue load after applying the impact energy

Based on the Paris–Erdogan equation [5], the crack growth rate against the variation of stress intensity factors were produced for *SE (B)* specimens made of *EA4T* forged steel. The constants of the model, i.e. parameters *C* and *m* in the equation were obtained from the experimental data by calibrating results to the Paris–Erdogan representative equation.

Results obtained following these procedures for arrange of experiments are summarized in Fig 4.

3. Discussion

Experimental results revealed that the application of impact load above a certain level, a minimum threshold, before being followed by fatigue loading changed the fatigue behaviour of the specimens. Table 5 shows the threshold stress intensity factor ranges ΔK_{th}, as well as the median lines, *Mcr,* approximating the experimental data points at crack growth rates.

Impact loads (corresponding to input energy levels between *0.5 ~ 3 J*) decreased the density of the pores and the size of the grains. Reduction of the grain size leads to an increase of the flow stress as well as the strain rate sensitivity. The flow stress is linearly related to the natural logarithm of the strain rate for strain rates ranging from approximately 10^{-3} to $10^{3}s^{-1}$ [20].

High strain rate tests have demonstrated that many metallic materials show distinct strain rate sensitivity following a change in their corresponding deformation mechanisms [21, 22]. It is also well known that reduction of the grain size and an enlargement in the obstacle effect of a grain boundary increase the fatigue life [23]. On the other hand, impact loading can well be responsible for the creation of micro cracks. In the initial steps of the fatigue loading, micro cracks decrease the magnitude of the crack growth rate. As a result, the Paris–

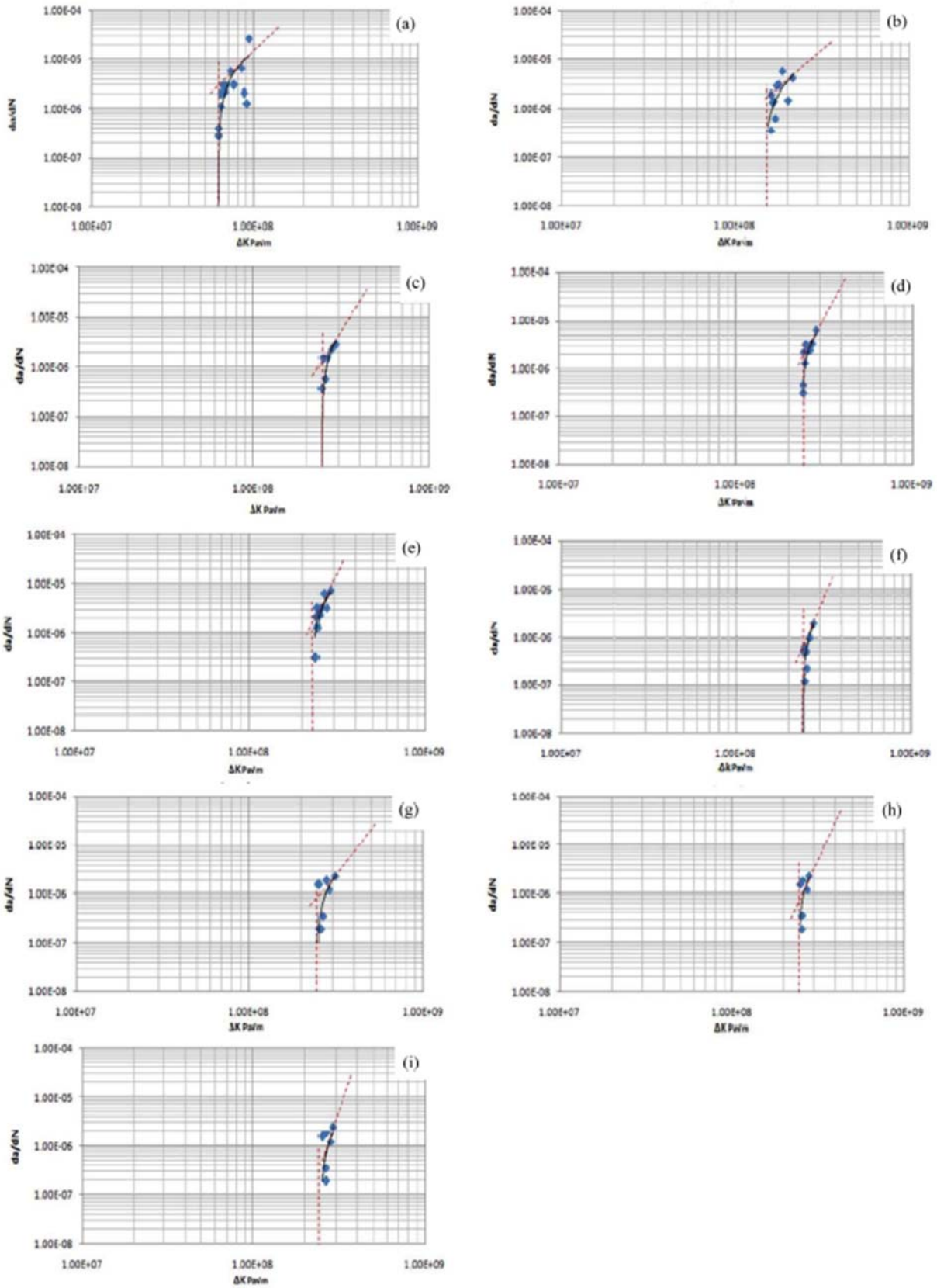

Fig. 4. Experimental results of the applying fatigue load after input energy of: (a) *0.5 J*; (b) *0.8 J*; (c) *1.0 J*; (d) *1.3 J*; (e) *1.6 J*; (f) *2.0 J*; (g) *2.3 J*; (h) *2.6 J*; (i) *3.0 J*.

Erdogan diagram shifts to right (grain size effect) and down (micro cracks effect).

Table5
Variations the threshold stress intensity factor ΔK_{th} and *Mcr*

Impact Energy (J)	ΔK_{th} (MPa$\sqrt{m}$	Mcr* (da/dN)
0.0	30	2.5e-6
0.5	60	2.9e-6
0.8	160	1.7e-6
1.0	235	1.3e-6
1.3	230	1.2e-6
1.6	240	1.6e-6
2.0	242	8.5e-7
2.3	246	7.5e-7
2.6	250	6.5e-7
3	254	4.5e-7

Table 6
Variations of the constants C and m on the Paris equation

Impact Energy (J)	C	m
0.0	2.97e-10	3.2
0.5	1.44e-10	3.4
0.8	1.67e-11	3
1.0	9.85e-12	3.2
1.3	6.90e-12	3.2
1.6	8.10e-12	3.4
2.0	6.55e-13	3.4
2.3	4.03e-13	3.4
2.6	9.96e-14	3.8
3	9.50e-14	3.8

Based on the Paris-Erdogan Eq. (6) and the experimental results (Fig. 4), constants *C* and *m* were calculated for every combination of loading conditions. The variations of the constants *C* and *m* are presented in Table 6 and Fig. 5.

$$(da/dN) = C(\Delta K)^m \quad (6)$$

As these results suggest, the variation of exponent *m* is in the range of *3 ~ 3.8* whereas the coefficient C ranges *2.97e-10 ~ 9.50e-14*. The trend of variation of the constants *m* and *C* may be represented by introducing the approximate functions of the forms shown in Eqs. (7) and (8):

$$m = 0.25U + 3 \quad (7)$$

$$C = 10^{-11} \times U^{-4.08}. C = 10^{-11}. U^{-4.08} \quad (8)$$

where *U* is the input impact energy prior to fatigue loading.

Due to the significant plastic deformation in specimens subjected to the impact loads above *3 J*, the variation of the constant *C* is very small, i.e. equal to *9.50e-14*.

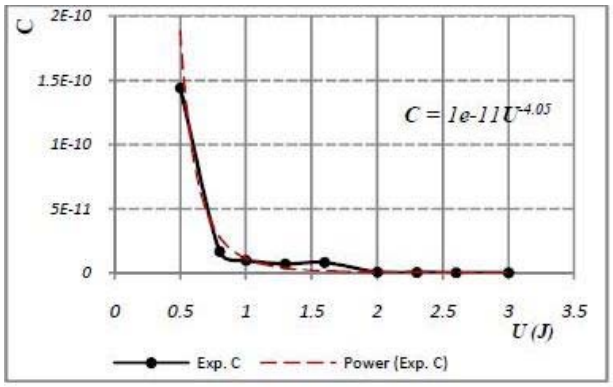

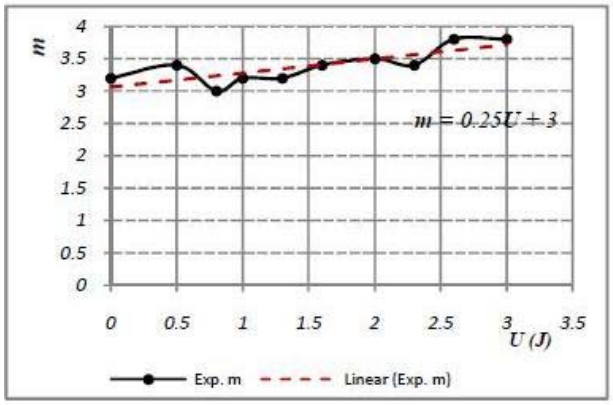

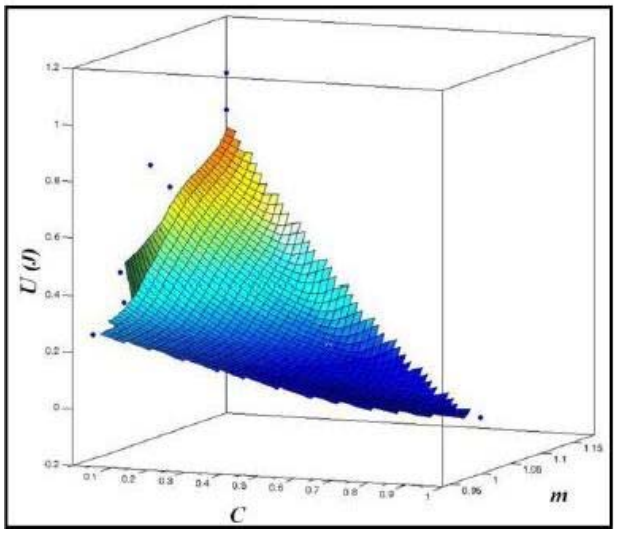

Fig 5. Variations of the constants *C* and *m* in Paris–Erdogan equation

4. Conclusions

SE (B) specimens of Forged steel *EA4T* were primarily subjected to various levels of prescribed impact loading. A small rig was designed and fabricated for this purpose. All specimens pre-impact loaded in this rig were then subjected to cyclic loading to fracture. The pre-impact loads of up to 0.5 Jules, showed no influence on the fatigue behavior when subjected to cyclic loading. However, the application of the higher impact energy caused a decrease in the fatigue life and time to fracture of the specimens. Also, results suggested that pre-

impact loading resulted in increasing ΔK as well as the rate of crack growth and shifted the Paris–Erdogan fatigue curve to the right and downward on the da/dN vs ΔK diagrams.

Therefore, an empirical model was adopted that modifies the parameters C and m to account for the observed shift in the results. The model predicts how pre-impact loading affected the fatigue characteristics of the specimens. The model parameters were calibrated using the experimental data. The proposed relationships describe C and m in terms of the input impact energy, U. The proposed model may be used as design tool to predict the behavior of this steel under combined impact and fatigue loading conditions.

Acknowledgment

This work was supported by the School of Engineering of Ferdowsi University of Mashhad, Iran.

Nomenclature----------

a/W : Normalized crack length
a : Crack length
B : Specimen thickness
BN : Specimen thickness between the roots of the side grooves
C : Constant of Paris-Erdogan equation
E : Effective Young's modulus (E/(1 − υ2) for plane strain)
f : Fatigue loading frequency
K : Stress intensity factor
L : Length of crack growth specimen
M : Constant of Paris-Erdogan equation
N : Number of load cycles
P : Applied force
$Pmean$: Mean load
$Pamp$: Amplitude load
PQ : Force as determined ASTME399 standard
S : Span of specimen supports
U : Input impact energy
Vm : Crack mouth opening displacement
W : Width of crack growth specimen
Mcr : Median line of crack growth zone
ΔKth : Threshold stress intensity factor
ΔK : Cyclic stress intensity factor
σyp : Yield stress
σult : Maximum tensile stress
da/dN : Crack growth rate

References

[1] I. Nonaka, S. Sectowaki and Y. Lchikawa, Effect of load frequency on high cycle fatigue strength of bullet train axel steel, *International Journal of Fatigue*, 60 (2014) 43-47.

[2] M. Luke, I. Varfolomeev, K. Lutkepohl and A. Esderts, Fatigue crack growth in railway axels: assessment concept validation tests, *Engineering Fracture Mechanics*, 78 (2011) 714-730.

[3] I. Varfolomeev, M. Burdack and M. Luke, Fracture mechanics as a tool for specifying inspection intervals of railway axels (part 2), *39. Tagung des DVM- Arbeitskreises Bruchvorgange,* Dresden, DVM-Bericht, 239 (2007) 33-42.

[4] P. Johnon, X. P. Zhang and G. Pluvinage, Crack growth rate in impact fatigue and in programmed variable amplitude loading fatigue, *Engineering Fracture Mechanics*, 37 (3) (1990) 519-525.

[5] H. Iguchi, K. Tanaka and S. Taira, Failure mechanisms in impact fatigue of metals, *Fatigue of Engineering Material and Structure,* 2 (3) (1979) 165-179.

[6] A. A. Johnson and R. J. Storey, The impact fatigue properties of iron and steel, *Journal of Sound and Vibration,* 308 (2007) 458-466.

[7] T. E. Stanton and L. Bairstow, The resistance of materials to impact, *Proceedings of the Institute of Mechanical Engineering* (1908) 889-919.

[8] D. J. McAdam Jr., Endurance properties of steel: Their relation to other physical properties and to chemical composition, *Proceedings of ASTM,* 23 (2) (1923) 56-105.

[9] A. A. Johnson and D. J. Keller, The impact fatigue properties of pearlitic plain carbon steels, *Fatigue of Engineering Material and Structure,* 4 (3) (1981) 279-285.

[10] D. N. Johnson and A. A Johnson, The low cycle impact fatigue properties of pearlitic plain carbon steels, *Fatigue of Engineering Material and Structure,* 8 (3) (1985) 287-294.

[11] L. R. Freund and J. R. Rice, On the determination of elastodynamic crack tip stress fields, *Int. J. Solids Struct*., 4 (1974) 293-299.

[12] V. Z. Parton and V. G. Boriskovsky, *Dynamic Fracture Mechanics*, Stationary Cracks (Edited by R. B, Hetnarski), Hemisphere Pub. Co., 1 (1989).

[13] P. Boresi and R. J. Schmidt, *Advanced mechanics of materials*, 6th Ed., Wiley (2003).

[14] P. C. Paris and F. Erdogan, A critical analysis of crack propagation laws, *Trans. ASME J. Basic Engng.*, 85 (1963) 528-534.

[15] ASTM Standard E0008, Test methods for tension testing of metallic materials, *Annual Book of ASTM Standards*, 03.01 (2009).

[16] ASTM Standard E2248-09, Test methods for notched bar impact testing of metallic materials, *Annual Book of ASTM Standards,* 03.01 (2009).

[17] ASTM Standard E 399, Test method for linear-elastic plane-strain fracture toughness *KIc* of metallic materials 1, *Annual Book of ASTM Standards,* 03.01 (2009).

[18] ASTM Standard E436-91, Standard test methods for dropweight tear tests of steels, *Annual Book of ASTM Standards*, 03.01 (1997).

[19] ASTM Standard E 1290-93, Test method for crack-tip opening displacement (CTOD) fracture toughness measurement, *ASTM*, 03.01 (2009).

[20] W.-S. Lee, C.-F. Lin and T.-J. Liu, Impact and fracture response of sintered 316L stainless steel subjected to high strain rate loading, *Materials Characterization,* 58 (2007) 363-370.

[21] G. Regazzoni, U. F. Kocks and P. S. Follansbee, Dislocation

kinetics athigh strain rates, *Acta Metall*, 35 (1987) 2865-2875.
[22] F. J. Zerilli and R. W. Arsmstrong, The effect of dislocation drag on the stress-strain behaviour of F. C. C. metals, *Acta Metall*, 40 (1992) 1803-1808.
[23] Y. Hong, Y. Qiao, N. Liu and X. Zheng, Effect of grain size on collective damage of short cracks and fatigue life estimation for a stainless steel, *Fatigue & Fracture of Engineering Materials & Stractures,* 21 (1998) 1317-1325.